# *iVRIDA*: intelligent Vehicle Running Instability Detection Algorithm for high-speed rail vehicles using Temporal Convolution Network – A pilot study

Rohan R Kulkarni, Rocco Libero Giossi, Prapanpong Damsongsaeng, Alireza Qazizadeh and Mats Berg

*Department of Engineering Mechanics, KTH Royal Institute of Technology, SE 100 44, Stockholm, Sweden*
rohank@kth.se

## ABSTRACT

Intelligent fault identification of rail vehicles from onboard measurements is of utmost importance to reduce the operating and maintenance cost of high-speed vehicles. Early identification of vehicle faults responsible for an unsafe situation, such as the instable running of highspeed vehicles, is very important to ensure the safety of operating rail vehicles. However, this task is challenging because of the nonlinear dynamics associated with multiple subsystems of the rail vehicle. The task becomes more challenging with only accelerations recorded in the carbody where, nevertheless, sensor maintenance is significantly lower compared to axlebox accelerometers. This paper proposes a Temporal Convolution Network (TCN)-based intelligent fault detection algorithm to detect rail vehicle faults. In this investigation, the classifiers are trained and tested with the results of numerical simulations of a high-speed vehicle (200 km/h). The TCN based fault classification algorithm identifies the rail vehicle faults with 98.7% accuracy. The proposed method contributes towards digitalization of rail vehicle maintenance through condition-based and predictive maintenance.

## 1. INTRODUCTION

Vehicle hunting motion (running instability) is an important phenomenon in vehicle-track dynamic interaction and typically appears at a fairly high vehicle speed and on a straight track or in large-radius curves. The running instability is an intrinsic behaviour of a vehicle system that is dependent on the health of the vehicle and track subsystems. The foremost reasons of running instability are poor vehicle yaw dampers, too soft primary suspension in the horizontal plane or poor wheel-rail interface geometry. Vehicle hunting is a safety concern and can also cause passenger discomfort. The European Standard *EN 14363:2016+A1* (2019) standard specifies the methods to measure vehicle running instability in the vehicle certification phase. However, these methods are not suitable for continuous health monitoring of the vehicle and track subsystems which influences the running instability of the vehicle. Gasparetto et al., (2013) employ Random Decrement Technique to extract the vehicle's hunting frequency and residual damping from bogie frame accelerations. These signal-based features are fed into k Nearest Neighbor (kNN) and Artificial Neural Network (ANN) fault classifiers to diagnose the reason behind the observed vehicle running instability, mainly vehicle-based faults. Ning et al., (2018), propose data-driven fault classifiers combined with data fusion of multiple bogie frame accelerations for diagnostics of vehicle hunting. The authors employ Empirical Mode Decomposition (EMD) and Sample Entropy (SE) methods to extract features associated with small amplitude hunting and incorporate them into Support Vector Machine (SVM) classifier as fault identifiers. Zeng et al., (2020) use a phase-space reconstruction algorithm to extract signal-based features to estimate the state variables periodicity in the nonlinear dynamic system and detect hunting based on axlebox accelerations. Kulkarni et al., (2019), deployed two classifiers (i.e., linear SVM and Gaussian SVM) for the Fault Detection and Isolation (FDI) of yaw dampers of high-speed trains. The simulation results showed that both classifiers could identify the faulty yaw dampers well. Moreover, the Gaussian SVM classifier performed slightly better in the training and testing phases, while it had a higher risk of overfitting the current dataset. Overall, the results showed the ability of the data-driven approach to be used for the FDI of railway vehicle suspension faults. The articles above, mainly extract features from axlebox acceleration or bogie frame acceleration and mainly use traditional machine learning algorithms. Moreover, these studies do not focus on intelligent fault identification of vehicle running instability.

The main objective of the present study is to detect vehicle running instability and identify the root causes from carbody floor acceleration using two different methods. Namely, Dynamic Mode Decomposition (DMD) (Brunton & Kutz, 2019) and Temporal Convolutional Neural Network (TCN) (Lea et al., 2016). The DMD method accurately estimates the eigenfrequencies and eigenmodes of the system. In recent times, a TCN is proposed which shows excellent abilities in solving sequential problems such as analysing time series data and outperforms Recurrent Neural Network (RNN) models. Thus, TCN is deployed to identify the root causes of observed vehicle running instability in this investigation. The iVRIDA algorithm is described in the next subsection which is followed by results and conclusions.

## 2. iVRIDA Algorithm

### 2.1. Algorithm Schematic

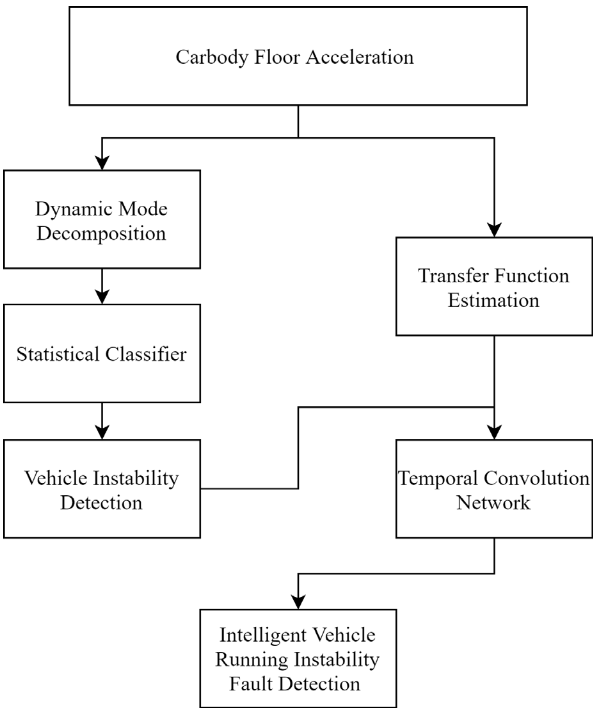


Figure 1 Schematic of iVRIDA algorithm

The proposed iVRIDA algorithm for vehicle running instability detection and root cause identification from carbody floor acceleration is illustrated in Figure 1. The algorithm utilizes two data-driven methods namely DMD and TCN aiming at detecting the vehicle instability and identifying root cause of the same. The hunting or vehicle running instability detection algorithm is implemented based on a binary classification method using outputs from DMD of carbody floor accelerations. Besides, the root causes identification is a classical multi-class classification problem and TCN is deployed on transfer functions between track and carbody floor.

### 2.2. Vehicle Running Instability Detection with DMD

The vehicle-track is a system where the nonlinearities mainly lie in the contact between the wheel and the rail. While hunting, a limit cycle is reached, and the system starts to oscillate at a certain frequency and with a precise mode shape. In this condition, an almost stable cycle can be detected. Thus, during hunting, the vehicle (bogies plus carbody) can be considered linear. This first assumption makes it possible to apply the DMD algorithm. Non-linearities are not expected in the time and spatial domains.

The DMD algorithm is chosen because it is a fast and accurate algorithm with which the eigenfrequencies and eigenmodes of the system can be detected. It is convenient in hunting detection due to the order in which the results are sorted, namely by energy content. In fact, in hunting motion, essentially only one mode will be excited. This mode will be the one with the highest energy content. It will be sufficient to consider the this mode.

The DMD algorithm assumes linear relation in time and space for the selected signals. The relation between the time $t_m$ and the previous one $t_{m-1}$ can thus be defined,

$$X\left(t_2,\ldots,t_m\right) = AX\left(t_1,\ldots,t_{m-1}\right) \rightarrow X_2 = AX_1, \qquad (1)$$

where, $X_1$ is the $n\times(m-1)$ matrix representing the state of the system at instances from $t_1$ to $t_{(m-1)}$, $X_2$ is the $n\times(m-1)$ matrix representing the state of the system at instances from $t_2$ to $t_m$ and $A$ is the state matrix. Here, $n$ is the number of sensors used and $m$ is the number of time steps. Applying the reduced Singular Value Decomposition (SVD) of the matrix $X_1$ with reduced order $r$,

$$X_1 = U_r\Sigma_r V_r^*, \qquad (2)$$

it is possible to estimate the state matrix $A$ to the reduced order $r$,

$$\hat{A} = U_r^* X_2 V_r \Sigma_r^{-1}. \qquad (3)$$

If the eigenvalue problem is solved for the matrix $\hat{A}$,

$$\hat{A}W = W\Lambda, \qquad (4)$$

It is now possible to determine the mode shapes $\Phi$ and the eigenfrequencies $f$ of the system,

$$\Phi = X_2 V_r \Sigma_r^{-1} W,\ f = \log\left(\Lambda\right) f_s, \qquad (5)$$

where, $f_s$ is the sampling frequency.

During the analysis, the DMD algorithm with second-order reduction applied to carbody acceleration was able to identify correctly the eigenfrequencies of the system. In contrast, with the mode shape isn't possible to distinguish between hunting and non-hunting scenarios due to the scaling of the mode shapes themselves. To solve the problem, the following equality is assumed,

$$R = \Phi b, \tag{6}$$

where $b$ is the scaling factor and $R$ is the signals $n \times 1$ RMS matrix. In this way, it is possible to incorporate the energy information carried by the whole considered signal in the mode shapes themselves. In Figure **2** the effect is shown for the first 25 test cases. After the scaling, the mode shapes can be used in conjunction with eigenfrequencies to distinguish hunting cases from non-hunting ones using a statistical fault classifier.

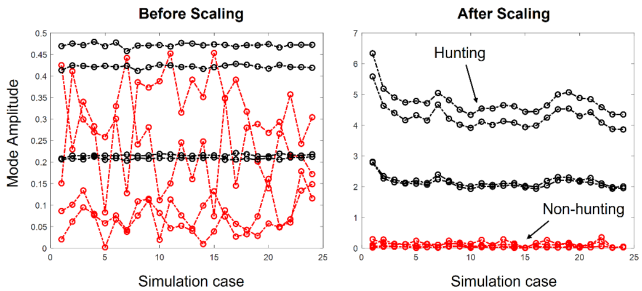


Figure 2 Effect of DMD mode shape scaling with signal RMS

## 2.3. Intelligent Fault Detection of Vehicle Running Instability with TCN

### 2.3.1. Estimation of Transfer Function

A rail vehicle running on track in presence of track irregularities can be considered a MIMO system, where Alignment Level (AL), Longitudinal Level (LL), Track Gauge (TG), and Cross Level (CL) are four input signals and vehicle accelerations in X, Y, and Z directions (i.e. longitudinal, lateral and vertical direction) are output signals. Thus, the transfer functions and coherence between carbody floor accelerations and track irregularities are estimated according to principals of MIMO system identification. The schematic of the MIMO system is shown in Figure **3** The simplified relationship between the input and output signal is modelled by linear, time-invariant Transfer Functions.

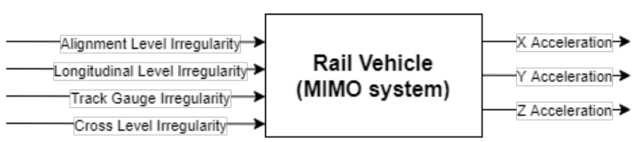


Figure 3 Modelling a Rail Vehicle as a MIMO system (A simplified schematic)

### 2.3.2. Transfer Function Estimation Case Study

In this case study, the EUROFIMA coach (Iwnicki, 1999) is running on a 2 km tangent track section in presence of AL, LL, TG, and CL irregularities. These track geometry irregularities are distributed among classes A, B and C defined in the European Standard *EN 13848-5:2017* (2017) standard and the irregularity signals are free from defects. The track irregularities are shown in Figure **4** (a-d). For simulations three different wheel-rail conditions are considered, see Table 1. In the three cases, a worn wheel profile (T19) is applied to all wheels of the coach. Two rail profiles, namely MS3_MS4 (ground rail) and BDL354U28 (worn rail) are applied to the rails. Case1: No fault at the wheel-rail interface; Case2: Tight gauge fault; Case3: worn rail profile fault (see Table **1**). Running equivalent conicity for the three simulation cases is shown in Figure 3(e). Case1: low conicity conditions; Case2: high conicity conditions caused by tight track gauge; Case3: high conicity conditions caused by worn rail profile.

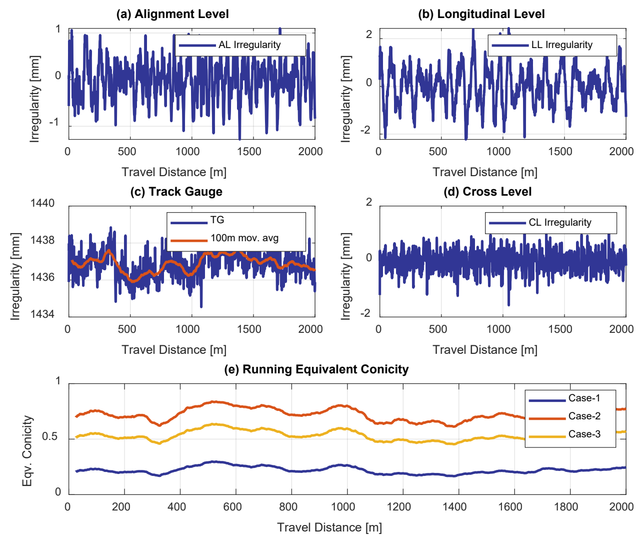


Figure 4 Track irregularities (a-d) and running equivalent conicity (e)

Table 1 Summary of Simulation Cases

| Case Number | Wheel Profile | Rail Profile | Avg TG Range [mm] |
|---|---|---|---|
| Case 1 | T19 | MS3_MS4 | 1436-1438 |
| Case 2 | T19 | MS3_MS4 | 1432-1434 |
| Case 3 | T19 | BDL354U28 | 1436-1438 |

The simulated vehicle response at the carbody floor (above the left axlebox of the leading wheelset) is stored in GENSYS. The differences between the three cases is shown by the X and Y accelerations of the carbody floor and EN 14363 stability evaluation (i.e., 100 m moving RMS of bandpass filtered lateral bogie frame acceleration) for the three simulated cases are shown in Figure **5**. In each subfigure abscissa and ordinate axes are travel distance and acceleration, respectively. In case1, X&Y acceleration amplitudes are low (see subfigure a, b) and the lateral bogie frame acceleration is much lower than the limit value (subfigure c). In case2, the vibration level is very large, especially the lateral acceleration (see subfigures d, e). The lateral bogie frame acceleration exceeds the threshold value on many occasions on this 2 km section as seen in subfigure (f). In case3, also the vibration level is strong and to the order of 0.8 m/s2 (see subfigures g, h). The lateral bogie frame acceleration is high but always lower than the threshold value throughout this 2 km section as seen in subfigure (i).

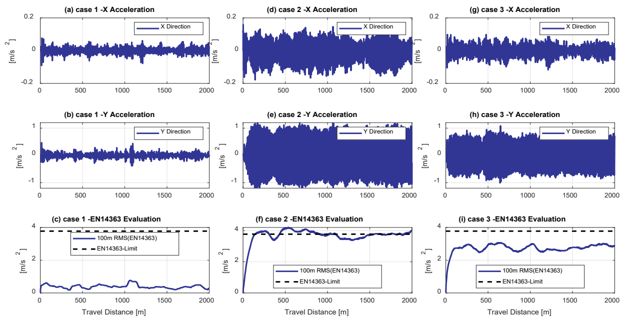


Figure 5 X, Y raw carbody floor accelerations and stability evaluation of bogie frame according to European Standard EN14363 scheme in case1, case2, and case3.

The lateral carbody floor acceleration is processed through the first feature extraction algorithm to obtain transfer functions. The transfer functions for Y & AL and Y & CL are shown in Figure **6**. The functions are presented as distance–frequency plots to obtain spatial and frequency localization of the vehicle behaviour. In each plot, abscissa and ordinate are travel distance and frequency, respectively, whereas the colour shows the transfer function's magnitude in dB scale. In case1, the magnitude of both transfer functions is always below 0 dB throughout the travel distance (see subfigures a, b). In case2, the Y vs AL transfer function (subfigure c) peaks in the 5-6 Hz range with amplitude above 30 dB and amplitude below 0 dB elsewhere. The magnitude of the Y vs AL transfer function does not change much throughout travel distance except for 200 m around the 1000 m marker. Similarly, the Y vs CL transfer function (subfigure d) of case2 exhibits peaks at 5-6 Hz with amplitude in the 0-10 dB range. In case3, the Y vs AL transfer function (subfigure e) peaks in the 5-6 Hz range with an amplitude of 10-20 dB throughout the travel distance. Similarly, the Y vs CL transfer function (subfigure f) of case3 does not exhibit strong peaks at 4-6 Hz.

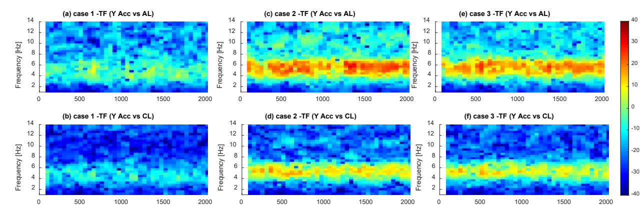


Figure 6 Transfer Functions between Y acceleration and AL & CL track irregularities for case1, case2 and case3

The magnitude of the transfer function between carbody floor and track at a particular frequency varies with time as the vehicle travels on track mainly because of variations in equivalent conicity. This varying magnitude of the transfer function at a specific frequency is time-series data and the transfer function contour plots shown above are a collection of time series which are highly nonlinear. This time-series data is used for the identification of root causes of observed vehicle running instability.

### 2.3.3. Temporal Convolutional Network (TCN)

A Convolution Neural Network (CNN) is a classical neural network that performs well at image processing tasks because of its excellent feature extraction capabilities. Currently, CNN hasbeen widely used in many fields such as face recognition, automatic driving, and security. However, CNN models are poor in extracting temporal features from the data. In recent times, a Temporal Convolutional Network (TCN) is proposed which shows excellent abilities in solving sequential problems such as analyzing time series data and outperforms Recurrent Neural Network (RNN) models. Thus, TCN is deployed to identify the root causes of observed vehicle running instability in this investigation.

Generally speaking, TCN has two main characteristics. Firstly, it maintains a causal relationship between each layer of the network, which means that the convolution output of a layer is determined solely on the convolution result of layers before. Thus, the data coherence and time coherence are better protected than the limited historical information storage and possible data absence of LSTM's memory cell. Secondly, the architecture of this model can be flexibly adjusted to any length. It can also be mapped according to several interfaces required by the output, which is similar to the RNN framework. Compared with the traditional CNN network structure, TCN adds four core parts to the design: sequence modelling, causal convolutions, dilated convolutions, and residual connections. This subsection will introduce the architecture and working principle through these four parts in brief.

1. Sequence Modelling: A simple sequence modelling task is used to illustrate the sequence modelling characteristics of TCN. If the input sequence is given, it requires predicting the specific outputs $O_0,.....,O_T$ at every step. Following the requirements, the model should predict the corresponding output at a particular time point. The key constraint of sequence modelling is that the output at a time should be generated by exactly the recorded inputs before time $t$ instead of the post-positional information, which follows the sequence of data flow. The one-to-one mapping from it to $y_t$ of sequence modelling network could be simply expressed as:

$$\hat{O}_0,...,\hat{O}_T = f(i_0,...,i_T) \tag{7}$$

2. Causal Convolutions: After the introduction of the sequence modelling above, two principles of TCN are summarized. First, the length of output after model prediction will always remain the same as the input length. Second, the TCN remains invisible to 'future' information and always depends on the previous inputs to complete the prediction. To maintain the first principle, the TCN utilizes the 1D fully-convolutional network (FCN). The core idea of FCN is adopting the zero-padding method to guarantee that each output layer keeps the same length and width as the input layer in the propagation of the network. As for the second principle, TCN utilizes causal convolutions to prevent future information leakage. Causal convolutions are abstracted to predict current output $y_T$ depending on previous inputs $x_0,...,x_T$ and previous layers' output $y_0,...,y_{T-1}$ to approach the actual value. The example of causal convolution is shown in Figure 7

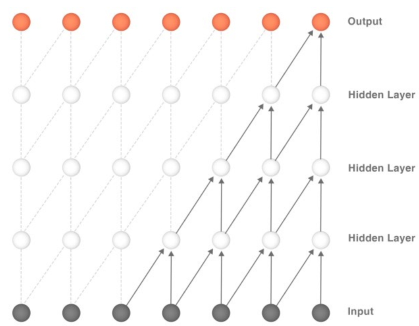

Figure 7 An example of causal convolutions

3. Dilated Convolutions: Although the above causal convolutional structure is feasible to prevent future information leakage, it increases the number of layers in the network and keeps extremely long historical information sequences simultaneously. As Figure 7 shows, the signed output in the upper right corresponds to five perceptive fields (5 grey balls in the input sequence), and it is obtained through five layers. It shows that the size of the receptive field has a positive linear correlation with the depth of the network, which may burden the learning process. To simplify the network and relieve memory storage pressure, TCN applies dilated convolutions on the network and forms an exponential correlation between the size of the receptive field and the number of layers. The following equation can demonstrate the principle:

$$F(s) = (x *_d f)(s) = \sum_{i=0}^{k-1} p(i) \cdot x_{s-d \cdot i} \tag{8}$$

Where d is the dilation factor and k is the filter size which $s-d \cdot i$ means convoluting only the former state. $x$ is the sequence input and $f:\{0,...,k-1\}$ is the filter. The operation $F$ takes the input s to complete convolutions using a fixed step between every two adjacent filter taps. Figure **8** shows the different dilated convolutions when $d$ is 1,2, and 4 respectively, the whole architecture of the network becomes dilated and includes less historical data. Therefore, this method can keep a large perceptive field with fewer layers and simplify learning tasks.

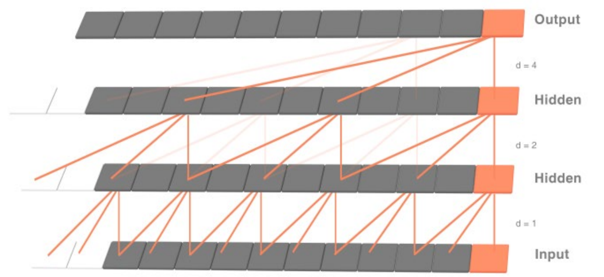

Figure 8 An example of dilated convolutions.

4. Residual Connections: The fast track in ResNet enables the model to learn the difference information, which effectively allows the network to modify the identity mapping to avoid gradient vanishing and gradient exploding problems in the deep layer model. For TCN, if the model needs to record a large amount of historical information, the final receptive field could be vast, and the network could become extremely deep. Hence, TCN adopted residual connections to reduce network depth. Each residual block module consists of two layers of residual convolutions, ReLU and batch normalization operation. In addition, spatial dropout is added after the activation function. An illustration of detailed residual block construction is in Figure **9**.

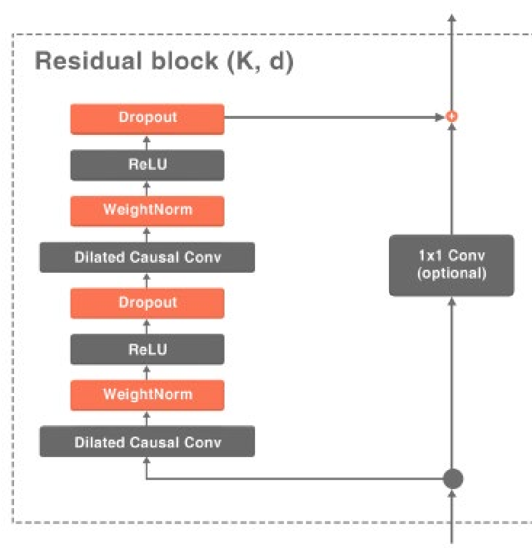

Figure 9 The profile of one residual block in TCN.

The advantages of TCN are -

1. TCN can conduct convolution operations in parallel. Therefore, TCN can preserve long-term memory in both training and validation.
2. Gradient stable TCN has a different backpropagation path from the sequence time direction, which avoids the gradient exploding and gradient vanishing problems in deep-layer networks compared to the RNN.
3. The TCN can possess a sizeable perceptive field under the condition of shallow layers. Therefore, TCN can be more flexible in the model's memory size, and it is easy to migrate to other fields.
4. The TCN can accept any length of the input sequence by sliding one-dimensional convolutional kernels. Therefore, it is flexible to be utilized on distinct tasks.

The disadvantages associated with TCN are -

1. To maintain the long-term memory and generate the predicted result, the TCN needs to occupy more memories during the testing phase.
2. When TCN migrates to different fields, the requirement of historical length and perceptive field will be distinct. Hence, migration operations could result in a weak expression of the TCN model.

## 3. Formulation of Vehicle Response Database

### 3.1. Vehicle Model

In this investigation, the hunting behaviour of a vehicle is investigated using the commercial multibody dynamics software GENSYS (AB DEsolver) by performing time domain simulations. The Swedish train operator SJ operates the fast trains X2000 on the Swedish rail network. Most SJ X2000 trains consist of a power car, five intermediate coaches and a driving trailer and are operating at a top speed of 200 km/h. An intermediate coach is modelled here in GENSYS. The vehicle model consists of a carbody, two bogie frames and four wheelsets which are modelled as 6 DOF rigid bodies and connected by primary and secondary suspension elements. The primary and secondary suspensions consist of spring and viscous damper elements in the x, y, and z-directions. Since the X2000 coach is specifically designed to run in curves at high cant deficiencies, the primary suspension is relatively soft to give the wheelsets improved radial self-steering capabilities. The X2000 coach model is also equipped with four yaw dampers as shown in Figure 10 i.e., two per bogie, which works in the longitudinal direction.

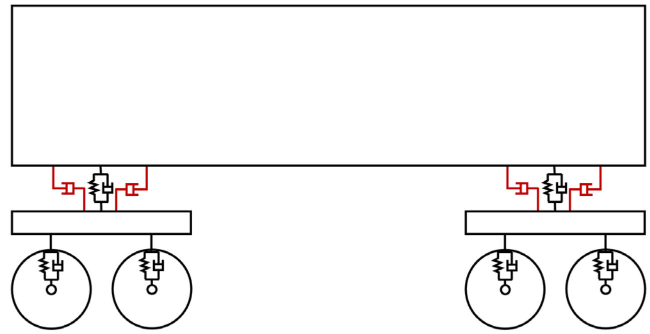

Figure 10 Schematic of MBS model of rail vehicle (Side view)

### 3.2. Vehicle Dynamic Simulations

Vehicle running instability can be caused by various parameters such as poor conditions of track gauge, suspension components and wheel-rail interfaces. In this investigation, the simulations are carried out with variation of wheel-rail friction, equivalent conicity and yaw damper as these factors mainly affect the running stability. Therefore, 384 simulation cases were performed with the combination of 3 friction values, 8 conicity cases and 2 damping coefficients for each yaw damper as summarized in Table 2. In total 384 cases are obtained with a full factorial design of the 6 parameters.

Table 2: Simulation Parameters

| Parameter | Values |
|---|---|
| Friction | 0.1, 0.35, 0.6 |
| Conicity | 0.1, 0.2, 0.3, 0.4, 0.5, 0.6, 0.7, 0.8 |
| Damping coefficient of yaw damper | 10% and 100% of the designed value |

The vehicle dynamic responses are measured with two accelerometers at two distinct diagonal locations on the carbody floor as illustrated in Figure **11**. The data obtained from these simulations are used for implementing the proposed iVRIDA algorithm.

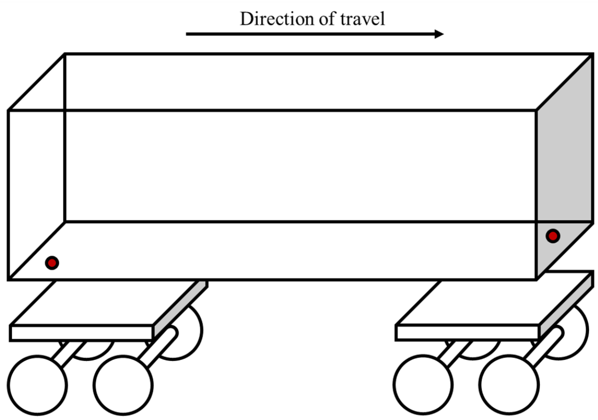


Figure 11 Sensor locations for acceleration measurements

### 3.3. Machine Learning problem formulation

#### Vehicle Running Instability Detection with DMD

The 3 features obtained from the DMD analysis of 384 cases, namely frequency and normalized mode shapes (at two sensor locations) are used for training and testing the fault classifier. The true labels are generated using the running instability evaluation scheme defined in EN14363. The EN 14363 scheme is typically used in the railway industry to classify the running state of the vehicle as stable or instable, thus this is a typical binary classification problem, and any typical statistical classifier can perform the above-mentioned classification task. Thus, in this investigation, Linear SVM is deployed. The database of 384 cases is divided with random stratification into training and testing datasets with 87.5% and 12.5% cases respectively. The Linear SVM (L-SVM) classifier is trained on a training dataset with 7-fold crossvalidation and the hyperparameters of the L-SVM are optimized. The results are presented in the result section.

#### Intelligent Fault Detection of Vehicle Running Instability with TCN

The time-series form of transfer functions as explained in 2.3.2 of each case are used for the identification of root causes of observed vehicle running instability using TCN. The time series of all 384 cases are horizontally stacked together to obtain a very large matrix. This large collection of time series of 384 cases is used for training and testing the TCN. The true labels corresponding to each case are obtained from the simulation parameters. The simulations with a 10% damping coefficient of the yaw dampers are labelled as yaw damper faults. There are 16 classes of yaw damper fault conditions as there are four yaw dampers in the vehicle and one or more may fail simultaneously. Thus, this is a typical multiclass classification problem. The database of 384 cases is randomly divided with stratification into training and testing datasets with 87.5% and 12.5% cases respectively. The training dataset is stratificaly divided into 7 folds and the first 6 folds formed 6 batches for the training of TCN. The last 7th fold is used as the validation set and the best performing TCN on the validation dataset is tested on the test dataset.

## 4. Results

### 4.1. Vehicle Running Instability Detection with DMD

The DMD algorithm is applied to the simulation cases described in subsection 3.2 The results are shown in **Figure 12**, subfigure a & b corresponds to instable cases and subfigures c & d to stable cases. Subfigures a & c shows the carbody vibration frequency of instable and stable cases whereas subfig b & d shows corresponding normalized mode shapes. It can be seen, two distinct families corresponding to instable and stable cases are now distinguishable. In the mode shape of the hunting cases, it is now possible to distinguish which part of the carbody is most excited, front (_111_), rear (_122_) or both.

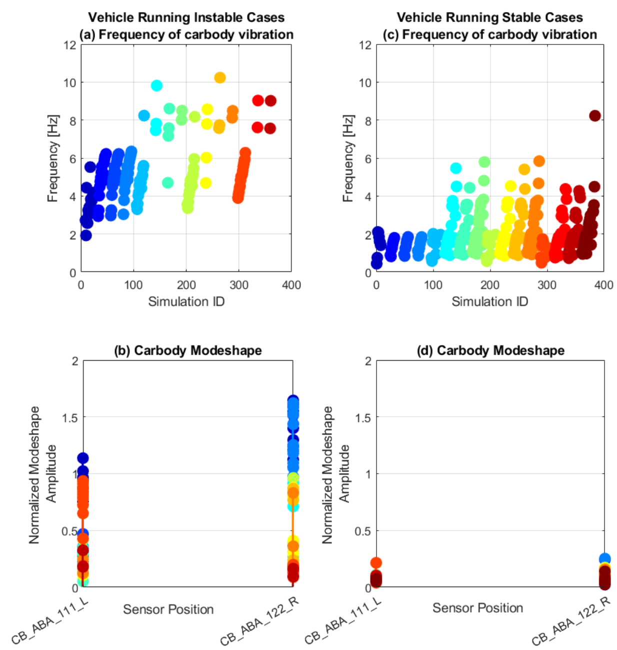


Figure 12 Frequencies and mode shapes for instable and stable cases detected with the DMD algorithm

The performance of the L-SVM classifier on the DMD dataset is shown as a confusion matrix in **Figure 13**, subfigure a & b show the performance of LSVM in the training and testing phase respectively. The LSVM classifies all cases with 100% accuracy in both the training and testing phase.

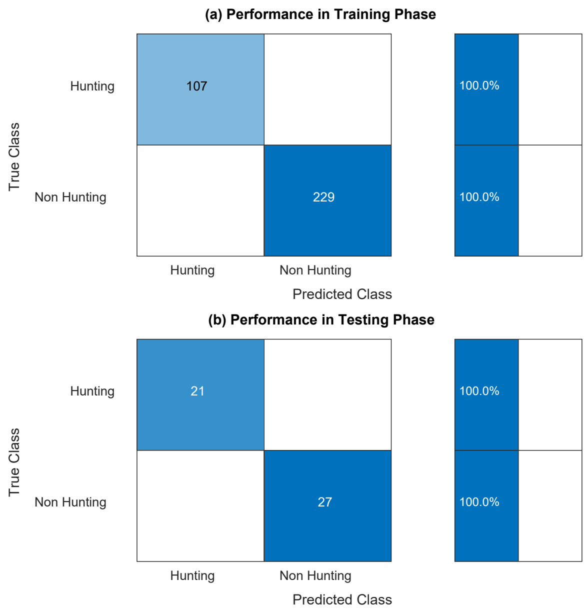


Figure 13 Detection of vehicle running instability with DMD+LSVM

## 4.2. Intelligent Fault Detection of Vehicle Running Instability with TCN

The performance of TCN in this investigation is evaluated with help of a confusion matrix where true labels are on the y-axis and predicted labels on the x-axis. The row-wise performance is summarised on the right-hand side of the respective confusion matrix. The results obtained during the testing phase are presented in Figure 14, and the trained fault classifier identifies root causes with 98.7% accuracy.

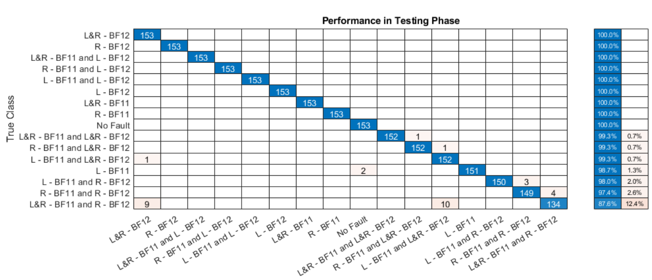


Figure 14 Intelligent Fault Detection of Vehicle Running Instability with TCN

The comparison of predicted fault labels and true fault labels is shown in Figure 15. In the figure, the x-axis is the test observation ID, the y-axis is the fault labels. The true fault labels are shown with a blue line and predicted labels with a black solid circle. In the well-trained fault classifier, ideally, the black solid circles should follow the blue line. It can be observed in the figure that the TCN fault classifier's performance is very accurate across the whole test sequence except a few misclassifications.

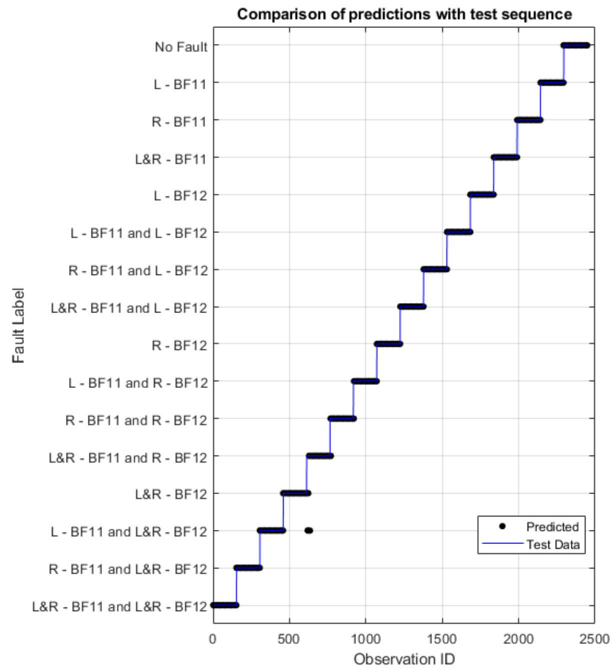


Figure 15 Comparison of predicted labels with true labels in the test sequence

## 5. CONCLUSIONS

In this paper, a data-driven intelligent vehicle running instability detection method is proposed for detecting and identifying the root cause of vehicle running instability of fast railway vehicles. The proposed novel methodology utilises carbody floor accelerations for intelligently detecting the vehicle faults exciting vehicle running instability. The iVRIDA algorithm detects vehicle running instability with the DMD+SVM method and corresponding root causes with Temporal Convolutional Network (TCN). In this investigation, both fault detection models are trained and tested with an extensive database generated with numerical experiments. The DMD+SVM algorithm detects the stability of high-speed rail vehicles from carbody floor accelerations with 100% accuracy. The TCN based fault classifier identifies the root cause of running instability with 98.7% accuracy. Thus, it is significant that iVRIDA detects and isolates the occurrence of vehicle running instability and corresponding root cause from carbody floor accelerations. The most important benefit of the proposed novel deep learning algorithmis the enhancement in obtaining a reliable Intelligent fault detection method with minimal sensor maintenance.

## 6. References

AB DEsolver. (n.d.). *GENSYS: A software tool for modelling and simulating vehicles running on rails*. http://gensys.se/

Brunton, S. L., & Kutz, J. N. (2019). Data-Driven Science and Engineering. In *Cambridge University Press*. Cambridge University Press. https://doi.org/10.1017/9781108380690

*EN 13848-5:2017 - Railway applications – Track – Track geometry quality – Part 5: Geometric quality levels – Plain line, switches and crossings*. (2017).

*EN 14363:2016+A1 - Railway applications – Testing and simulation for the acceptance of running characteristics of railway vehicles – Running behaviour and stationary tests*. (2019).

Gasparetto, L., Alfi, S., & Bruni, S. (2013). Data-driven condition-based monitoring of high-speed railway bogies. *International Journal of Rail Transportation*, *1*(1), 42–56. https://doi.org/10.1080/23248378.2013.790137

Iwnicki, S. (1999). The Manchester Benchmarks for Rail Vehicle Simulation. In S. Iwnicki (Ed.), *Vehicle System Dynamics* (Vol. 31, Issue Supplement).

Kulkarni, R., Qazizadeh, A., Berg, M., & Stichel, S. (2019). Fault Detection and Isolation Method for Vehicle Running Instability from Vehicle Dynamics Response Using Machine Learning. *Proceedings of BOGIE'19*.

Lea, C., Vidal, R., Reiter, A., & Hager, G. D. (2016). Temporal convolutional networks: A unified approach to action segmentation. In *Lecture Notes in Computer Science (including subseries Lecture Notes in Artificial Intelligence and Lecture Notes in Bioinformatics): Vol. 9915 LNCS* (pp. 47–54). https://doi.org/10.1007/978-3-319-49409-8_7

Ning, J., Liu, Q., Ouyang, H., Chen, C., & Zhang, B. (2018). A multi-sensor fusion framework for detecting small amplitude hunting of high-speed trains. *Journal of Vibration and Control*, *24*(17), 3797–3808. https://doi.org/10.1177/1077546318787945

Zeng, Y., Zhang, W., & Song, D. (2020). A new strategy for hunting alarm and stability evaluation for railway vehicles based on nonlinear dynamics analysis. *Proceedings of the Institution of Mechanical Engineers, Part F: Journal of Rail and Rapid Transit*, *234*(1), 54–64. https://doi.org/10.1177/0954409719830177